CRYSTAL GROWTH & DESIGN

Article

pubs.acs.org/crystal

Thermal Behavior of Benzoic Acid/Isonicotinamide Binary Cocrystals

Asma Buanz,[†] Timothy J. Prior,[‡] Jonathan C. Burley,[§] Bahijja Tolulope Raimi-Abraham,[†] Richard Telford,[∥] Michael Hart,[⊥] Colin C. Seaton,[∥] Philip J. Davies,[#] Ian J. Scowen,[¶] Simon Gaisford,*[,†] and Gareth R. Williams*[,†]

[†]UCL School of Pharmacy, University College London, 29−39 Brunswick Square, London WC1N 1AX, U.K.

[‡]Department of Chemistry, University of Hull, Cottingham Road, Hull HU6 7RX, U.K.

[§]Laboratory of Biophysics and Surface Analysis, Boots Science Building, School of Pharmacy, University of Nottingham, University Park, Nottingham NG7 2RD, U.K.

[∥]School of Chemistry and Forensic Sciences, Faculty of Life Sciences, University of Bradford, Bradford BD7 1DP, U.K.

[⊥]Diamond Light Source, Harwell Science & Innovation Campus, Didcot OX11 0DE, U.K.

[#]TA Instruments, 730−740 Centennial Court, Centennial Park, Elstree WD6 3SZ, U.K.

[¶]School of Chemistry, University of Lincoln, Brayford Pool, Lincoln LN6 7TS, U.K.

Supporting Information

ABSTRACT: A comprehensive study of the thermal behavior of the 1:1 and 2:1 benzoic acid/isonicotinamide cocrystals is reported. The 1:1 material shows a simple unit cell expansion followed by melting upon heating. The 2:1 crystal exhibits more complex behavior. Its unit cell first expands upon heating, as a result of C−H···π interactions being lengthened. It then is converted into the 1:1 crystal, as demonstrated by significant changes in its X-ray diffraction pattern. The loss of 1 equiv of benzoic acid is confirmed by thermogravimetric analysis−mass spectrometry. Hot stage microscopy confirms that, as intuitively expected, the transformation begins at the crystal surface. The temperature at which conversion occurs is highly dependent on the sample mass and geometry, being reduced when the sample is under a gas flow or has a greater exposed surface area but increased when the heating rate is elevated.

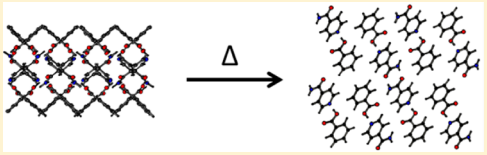

INTRODUCTION

Pharmaceutical cocrystals have attracted increasing research attention in recent years to ameliorate problems with solubility and physical and chemical stability.[1] The physical form of an active pharmaceutical ingredient (API) is integral in the determination of these properties, and control and understanding of this is of vital importance in the medicine development process. Metastable and amorphous physical forms offer rapid dissolution but suffer from the concomitant problem of potential conversion back to the most stable crystalline form, jeopardizing the therapeutic efficacy of the formulation. The preparation of salts (comprising the ionized API and a counterion) can yield accelerated dissolution, and this route has been widely explored.[2] Hydrates and solvates have additionally received much attention.[3]

Cocrystals, in which the neutral API is combined with a neutral coformer in a single crystalline phase, have been shown to be capable of improving physical, mechanical, dissolution, and bioavailability properties for a range of APIs.[4] For instance, the hygroscopicity of theophylline can be reduced through forming cocrystals with oxalic acid.[5] The bioavailability in dogs of 2-[4-(4-chloro-2-fluorophenoxy)phenyl]pyrimidine-4-carboxamide, a developmental sodium channel blocker, has been found to increase upon formation of a glutaric acid cocrystal.[6] In addition, cocrystal formation can solve challenges associated with bitter or unpleasant tasting APIs, for instance, by combining them with saccharin,[7] and can result in improvements in processability.[8,9] In favorable instances, two APIs may be combined in a cocrystal.[10] There are myriad examples of binary cocrystals in the literature,[4] and increasingly ternary systems are also being studied.[4,11] In order to drive effective cocrystal formation, it is important that there are strong intermolecular interactions between the crystal components. These may take the form of H-bonds, $\pi-\pi$ stacking interactions, or van der Waals forces. Increasingly, researchers are developing sophisticated ways of assessing the compatibility of coformers and systematically predicting which combinations will and will not form stable composite systems.[12−16]

Benzoic acid (BA) and isonicotinamide (isoNCT) have both been widely explored as coformers for pharmaceutical cocrystal synthesis.[17−21] They are known to form both 1:1 (BA/isoNCT)[22] and 2:1 (BA_2/isoNCT)[18] cocrystals. Possible synthetic routes to these include solution methods,[18,22] melt crystallization,[21,23] template synthesis using BA crystals as a substrate,[21] and thermal inkjet printing.[17] The structures of both BA/isoNCT and BA_2/isoNCT are given in Figure 1. In each case, there are hydrogen bonds between the benzoic acid and the pyridine function of the isonicotinamide. The 2:1

Received: March 13, 2015
Revised: May 18, 2015

DOI: 10.1021/acs.cgd.5b00351
Cryst. Growth Des. XXXX, XXX, XXX−XXX

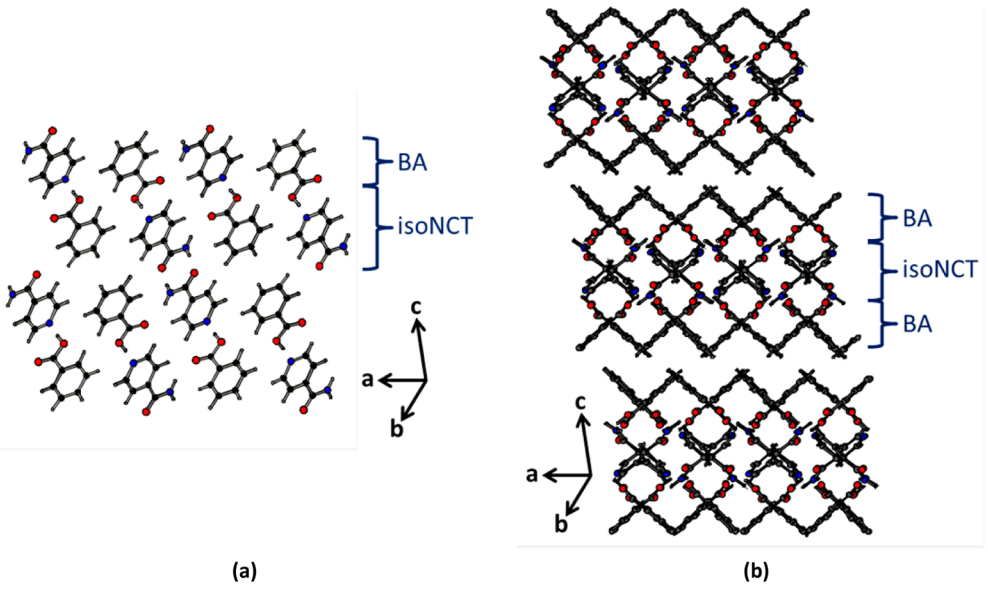

Figure 1. Structures of (a) BA/isoNCT and (b) BA_2/isoNCT.

material also contains hydrogen bonds between the BA COOH group and the isoNCT amide group, plus C−H···π contacts, while the 1:1 crystal features hydrogen bonds between the amide groups of adjacent isoNCT units.

It has been shown that both the stoichiometry and polymorphic form of binary pharmaceutical cocrystals can be varied through the synthetic conditions. For instance, polymers have been used to drive the formation of different polymorphs of the 2:1 adefovir/succinic acid cocrystal.[24] Synthesis at different temperatures results in different polymorphic 1:1 cocrystals of benzoic acid and pentafluorobenzoic acid.[25] The 1:1 form of a coumaric acid/nicotinamide cocrystal has been reported to be converted into a 2:1 material upon making a slurry in water;[26] the 1:1 urea−succinic acid system can similarly be converted to a 2:1 form when it is stirred in certain solvents.[27] Similar results been observed for the BA/isoNCT case: both the 2:1 and 1:1 cocrystals are stable in water, but in ethanol the 2:1 system is converted into a 1:1 material.[20]

Both Seaton and Buanz have separately reported that upon heating to 142−143 °C, the BA_2/isoNCT material is converted to BA/isoNCT.[17,21] This transformation involves the loss of one-third of the unit cell contents and a very significant reorganization of the coformer arrangement. It is hence remarkable that this conversion can take place. A few thermally induced cocrystal transitions are known beyond the BA/isoNCT system: for instance, the caffeine/theophylline cocrystal dissociates upon heating to yield a binary mixture of pure caffeine and theophylline.[28] Similarly, two 1:1 nicotinamide/pimelic acid cocrystal phases are known and can be interconverted upon heating.[29]

Liquid-mediated transformations between cocrystal forms can be fairly easily understood in that dissolution/reprecipitation mechanisms can facilitate significant changes in molecular arrangements. Small changes in intermolecular interactions to yield slightly different polymorphs upon heating are also unsurprising, most likely being facilitated by thermal motions. The thermal transformation of BA_2/isoNCT to BA/isoNCT is, insofar as the authors are aware, the only thermally mediated cocrystal transition in which the stoichiometry of the material very profoundly changes. The transformation necessitates huge alterations in the ordering of the molecular components, and thus how the intermolecular interactions influence and are influenced by this transformation is of great interest. In addition, understanding such interactions and transformations will yield useful insight into the stability and design of pharmaceutical cocrystals. In this work, we endeavored to understand more about exactly how the BA_2/isoNCT to BA/isoNCT transformation occurs. In order to do so, a range of analytical techniques were applied to study the thermal behavior of both the 2:1 and 1:1 cocrystals and the thermally induced transformation between them.

MATERIALS AND METHODS

Synthesis. Benzoic acid (ACS reagent, ≥99.5%) and isonicotinamide (99%) were purchased from Sigma-Aldrich, U.K. BA and isoNCT at 1:2 and 2:1 molar ratios were used to prepare BA/isoNCT and BA_2/isoNCT, respectively. BA (0.2322 g) and isoNCT (0.5409 g) (for BA/isoNCT) or BA (0.2433 g) and isoNCT (0.1587 g) (for BA_2/isoNCT) were added to 50 mL of distilled water.[18] Solutions were prepared by heating to ca. 70 °C until complete dissolution had occurred, then allowing them to cool to room temperature and storing for at least 1 month. Crystals were collected by vacuum filtration and stored over silica gel in a desiccator for at least 24 h before characterization.

Characterization. *Hot Stage Microscopy.* Microscopy was initially carried out using a Zeiss Axioplan-2 microscope with a Linkham THMS600 hot stage controlled through the Axiovision software, with a linksys 32 patch for hot stage control. All microscopy was carried out under cross-polarization. Samples of BA_2/isoNCT were heated from 40 to 120 °C at 5 °C min^{-1} in an open crucible. Further microscopy studies were undertaken using a LeicaADM 2700 M microscope connected to a FP82HT Mettler Toledo Instruments heating stage unit and a FP90 Mettler Toledo Instruments central processor unit. Samples were heated from 40 to 150 °C at 2 or 10 °C min^{-1}. The Studio86 Design capture software (version 4.0.1) was used to record and capture thermal events in real time.

Time-Resolved in Situ X-ray Diffraction. Experiments were performed on Beamline I12 of the Diamond Light Source, U.K.[30] This beamline generates a continuous spectrum of X-rays over the energy range from 50 to 150 keV. All experiments reported here were conducted with the beam monochromated to an energy of ca. 53 keV (λ = 0.2337 Å). The Oxford-Diamond *In Situ* Cell (ODISC)[31] was employed to heat the samples. ODISC comprises an IR-heated furnace

DOI: 10.1021/acs.cgd.5b00351
Cryst. Growth Des. XXXX, XXX, XXX−XXX

system, and reactions were performed using ca. 0.5 g of material placed in a glass culture tube. The latter was mounted in a glassy carbon tube to ensure effective heat transfer. A Thales Pixium RF4343 detector was sited 2.5 m away from the reaction vessel. Diffraction patterns (4 s) were collected every 5 s.

Data were analyzed using the Fit2D program[32] to convert the 2D data collected on the Pixium to 1D patterns.[33] These patterns were background-subtracted using in-house routines, visualized in 3D using the Origin software (v9.1), and integrated using a second set of in-house routines (these fit a background to the data and then use Gaussian functions to model reflections and determine their areas). It was also possible to carry out LeBail fits and partial Rietveld fits to the observed data to extract structural information. The GSAS suite of programs was used for this.[34]

Variable Temperature Raman Spectroscopy. A LabRam HR Raman microscope/spectrometer was employed. A 50× lens was used to focus a 785 nm wavelength laser onto the sample. A grating of 600 lines mm^{-1} was employed to disperse the scattered light onto a Synapse 1024-pixel CCD thermo-electrically cooled to −70 °C. Spectra were collected for 2 s every 2 °C between 25 and 199 °C. The sample was maintained at a constant nominal temperature during data acquisition, and ramping between temperatures was set to be 10 °C min^{-1}.

Differential Scanning Calorimetry. Differential scanning calorimetry (DSC) measurements were performed on Q2000 and rapid heating (RHC) instruments (both TA Instruments). Calibrations for cell constant and enthalpy were performed with indium (T_m = 156.6 °C, ΔH_f = 28.71 J g^{-1}) according to the manufacturer's instructions. Nitrogen was used as the purge gas at a flow rate of 50 mL min^{-1}. TA aluminum pans and lids (Tzero) and heating rates of 10 °C min^{-1} were used for all experiments unless stated otherwise. Data were analyzed using the TA Instruments Universal Analysis 2000 software, and all transformation temperatures are reported as extrapolated onsets. The sample mass employed was ca. 5 mg for Q2000 DSC and 0.1 mg for RHC-DSC.

Thermogravimetric Analysis. Measurements were performed on a PerkinElmer Pyris-6 analyzer. Samples were heated at various rates in open ceramic pans using nitrogen as purge gas (flow rate = 20 mL min^{-1}). Data collection and analysis were performed using the Pyris software (version 3.81).

Thermogravimetric Analysis–Mass Spectrometry. Samples of the 2:1 BA_2/isoNCT cocrystal (ca. 5 mg) were loaded onto platinum pans and heated from room temperature to 180 °C at a constant heating rate of 10 °C min^{-1} under a helium purge gas (50 mL min^{-1}) using a TA Instruments Discovery TGA. Evolved gas analysis was performed throughout the experiment using mass spectrometry, with data acquired in scan mode (m/e 5−155) using a Pfeiffer Vacuum ThermoStar TM GSD 301 T mass spectrometer. Data were analyzed using the TA Instruments Universal Analysis Software

RESULTS

Hot Stage Microscopy. The transformation of the 2:1 BA_2/isoNCT material upon heating has been reported previously.[17,18,21] To obtain insight on how this process occurs on the macroscopic scale, hot-stage microscopy (HSM) was employed. HSM data collected at different temperatures during heating at 5 °C min^{-1} are presented in Figure 2.

In the HSM data, large columnar crystals of BA_2/isoNCT can be seen at 40 °C. They begin to transform at around 80−85 °C, when small needle-shaped crystals can be seen to appear on the surface of the brightly colored columns (an enlargement of Figure 2 is provided in the Supporting Information (Figure S1) to aid visualization). These needles increase in number as the sample is heated further, until the transformation appears complete at around 120 °C. Undertaking the HSM experiment at different heating rates clearly shows that the onset of the transformation both begins and appears to be complete at higher temperatures with more rapid heating (see Figure S2, Supporting Information). If the HSM experiment is repeated with the crystal surrounded by oil, small bubbles of what appear to be a gas can be seen exiting the crystal during heating (Figure S3, Supporting Information). The needles are believed to comprise the 1:1 BA/isoNCT cocrystal, as they are seen to persist above the melting point of BA (122 °C), as depicted in Figure S4, Supporting Information. If heating is continued above 125 °C, then the remaining material is observed to melt gradually over the approximate temperature range 130−160 °C, depending on the heating rate.

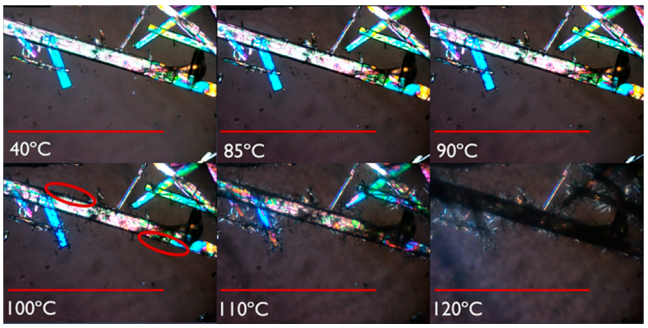

Figure 2. HSM data collected under crossed-polar conditions during the heating of BA_2/isoNCT at 5 °C min^{-1}. The red bar in each image represents 1 mm. The 120 °C image has been presented before in a previous study.[21] The rings in the 100 °C image highlight the needle-shaped crystals, which are present on the surface of the large columnar crystals.

***In Situ* X-ray Diffraction.** *The 1:1 Cocrystal.* The changes observed in the diffraction pattern of the 1:1 BA/isoNCT cocrystal upon heating from 30 to 179 °C at ca. 9.5 °C min^{-1} are depicted in Figure 3. As expected, the unit cell expands and reflections shift to lower angle upon heating. It should be noted that the intensity of the Bragg reflections fluctuates somewhat between temperatures: this appears to be a random effect that is tentatively ascribed to preferred orientation effects and the individual crystals comprising the sample repacking during the heating process.

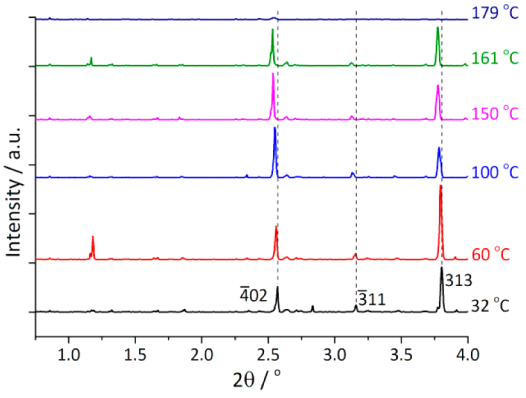

Figure 3. Evolution of the diffraction pattern for the BA/isoNCT 1:1 cocrystal with temperature.

The patterns may be satisfactorily indexed on expanded versions of the known cell for BA/isoNCT.[22] There is a steady increase in the a parameter with rising temperature (2.3% between 30 and 166 °C), a small increase (0.45%) in the b parameter, and decreases in c and β (0.43% and 0.35%, respectively). The cell volume increases in an approximately linear fashion with temperature, as does the a parameter

DOI: 10.1021/acs.cgd.5b00351
Cryst. Growth Des. XXXX, XXX, XXX−XXX

(Figure 4). The unit cells calculated at selected temperatures are detailed in the Supporting Information, Table S1. Partial

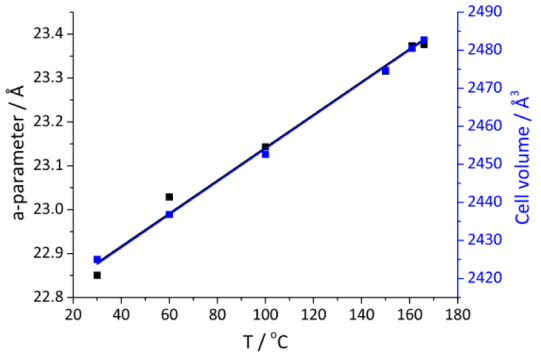

Figure 4. Variation in *a* parameter and unit cell volume observed on heating BA/isoNCT.

Rietveld fits are given in Figure S5, Supporting Information. Fitting of the observed data demonstrates that the structure of the 1:1 cocrystal does not undergo substantial molecular reorganization up to 161 °C. There is some evidence for a small amount of the 2:1 material being present as a trace impurity in the unheated BA/isoNCT.

At ca. 160 °C, the reflections begin to decrease in intensity as the material melts. This process is complete by 174 °C, after which there are no diffraction features present in the pattern.

The 2:1 Cocrystal. The evolution of the diffraction pattern of the 2:1 BA/isoNCT cocrystal was also recorded upon heating from room temperature to 179 °C at approximately 9 °C min^{-1}. The raw data collected are given in Figure 5. As the sample is heated, the characteristic reflections of the 2:1 crystal move to lower angle as a result of thermal expansion of the unit cell (see Figure 5b).

Below 150 °C, the diffraction patterns can be indexed on expanded versions of the previously reported cell for BA_2/isoNCT.[18] LeBail fitting was performed at selected temperatures, and the unit cells obtained are given in Table S2, Supporting Information. Partial Rietveld fits to the data may be found in Figure S6, Supporting Information. There is a gradual increase in the *a* parameter with rising temperature, while the *b* parameter remains essentially constant, and the *c* parameter expands much more profoundly (by 4.9% between 32 and 150 °C, cf. the *a* and *b* parameters, which change by 0.3% and −0.08%, respectively, over the same temperature range), as depicted in Figure 6. This can easily be rationalized in light of

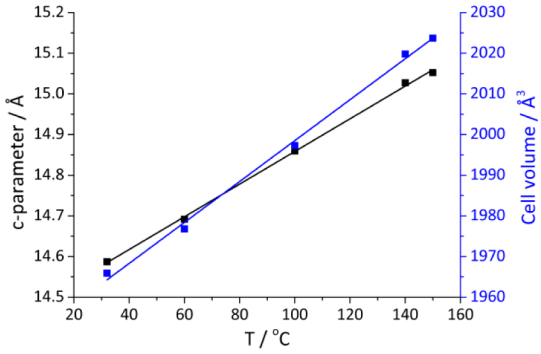

Figure 6. Variation in *c* parameter and unit cell volume observed on heating BA_2/isoNCT.

the structure of BA_2/isoNCT, which contains thick sections extending in the *ab* plane. These are held together in the *c* direction by C−H···π interactions. This weak interaction lengthens considerably upon heating, which is manifested principally in an expansion along the *c*-axis. The unit cell volume and *c* parameter both increase with temperature in an almost linear fashion (see Figure 6).

Above ca. 140 °C, some changes are apparent in the powder diffraction patterns of the 2:1 cocrystal. Most notably, the 001 reflection broadens, and by 150 °C, this is clearly composed of two peaks of roughly equal intensity that are very close together. It is possible to fit this with a single peak, but the pattern can better be fitted with a two-phase mixture (see Table S2 and Figure S6f, Supporting Information). A LeBail fit with two phases suggests that a smaller cell is evolving. Above 160 °C, the pattern is completely changed: at 161 °C, no trace of the 2:1 material can be seen. Upon continued heating to 179 °C, the system melts, and no diffraction peaks are visible.

The diffraction patterns of both the 2:1 and 1:1 crystals at 161 and 166 °C are shown in Figure S7, Supporting Information. The patterns obtained from both starting materials are virtually identical, demonstrating the similarity

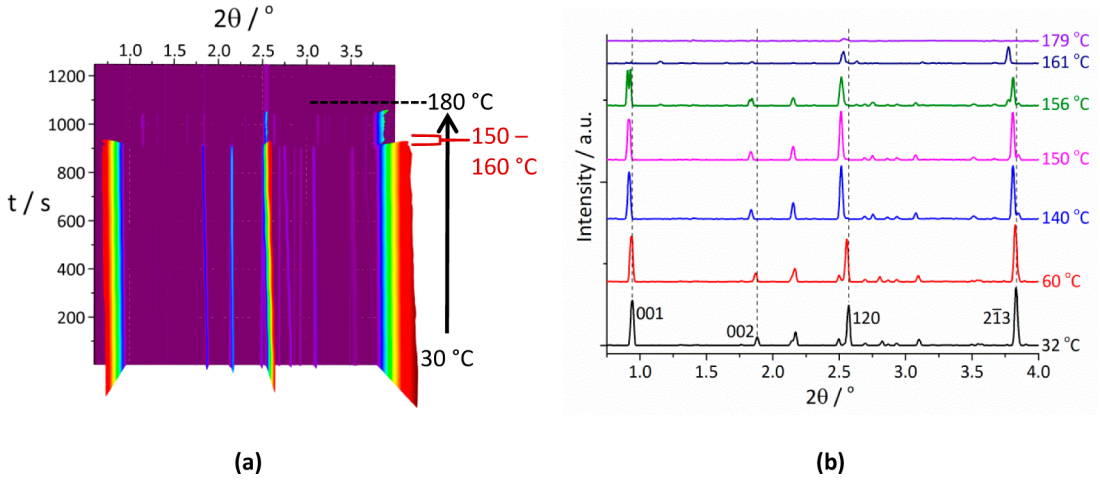

Figure 5. *In situ* XRD data recorded during heating of the 2:1 BA_2/isoNCT cocrystal: (a) 3D plot, and (b) selected diffraction patterns recorded at different temperatures.

DOI: 10.1021/acs.cgd.5b00351
Cryst. Growth Des. XXXX, XXX, XXX−XXX

Table 1. Unit Cell Parameters Calculated at 161 °C

starting material	*a*, Å	*b*, Å	*c*, Å	*β*, deg	*V*, Å^3
BA/isoNCT	23.373(5)	5.226(1)	20.431(6)	96.276(18)	2480.5(4)
BA_2/isoNCT	23.343(7)	5.225(2)	20.497(9)	96.370(30)	2484.6(6)

between crystalline components present in the two samples at these temperatures. Both the BA/isoNCT and BA_2/isoNCT systems are found to have virtually identical C-centered cells at 161 °C (see Table 1). The pattern from the 2:1 material is rather low intensity at 161 °C and above, but it is possible to perform a partial Rietveld fit to the observed data using the published crystal structure for the 1:1 cocrystal; this is shown in the Supporting Information, Figure S8. In terms of normal statistics, the fit is relatively poor, because of the narrow angular range and earlier background subtraction. However, visual inspection of the fit to the data shows that there is a single phase present: the 1:1 cocrystal.

This transformation is consistent with the emergence of a smaller unit cell when BA_2/isoNCT is heated above 150 °C. A loss of BA is needed for the interconversion to the 1:1 cocrystal. Structurally, both the *a* and *c* parameters change significantly. Within the 2:1 cocrystal, hydrogen bonded layers are stacked along [001]. BA projects above and below each layer. Loss of some BA upon heating would be expected to reduce the *c* parameter. Similarly there are C−H···π contacts between the layers that extend in the *xz* plane; directionally, these have no component along *b*. Thus, *a* and *c* change substantially as BA is lost but the *b* parameter does not vary much.

Selected reflections from each material were integrated, and the normalized intensity was plotted against temperature; the resultant data are presented in Figure 7.

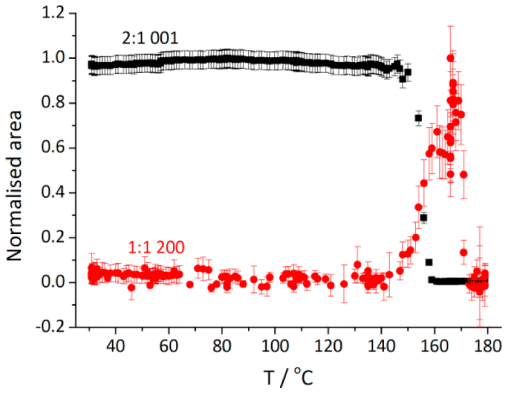

Figure 7. Changes in intensity observed with heating for selected reflections of the 2:1 and 1:1 BA/isoNCT cocrystals.

The area of the 2:1 001 reflection remains essentially constant until 150 °C, when it declines rapidly to zero. Concomitantly, the 1:1 200 reflection grows rapidly in intensity, reaching a maximum at 166 °C before then declining to zero again as the material melts. The normalized area vs temperature curves for the two species cross at approximately 0.5. This could be regarded as indicative of a direct solid−solid transition: as diffracted intensity is lost from the starting material, it is gained by the product. That said, it was clear from the HSM data that BA gas is evolved from the 2:1 cocrystal during transformation, and this gas could be involved in mediating the conversion.

Raman Spectroscopy. Both BA/isoNCT and BA_2/isoNCT were investigated using variable-temperature (VT) Raman spectroscopy, focusing on the lattice vibrations below 200 cm^{-1} since these will give most information on the molecular arrangements in the solid state.[35,36] The results of this analysis are presented in Figure 8. It is very clear that at ca. 150 °C there is an abrupt change in the features of the spectrum in the case of BA_2/isoNCT (red). Comparison of these data with those obtained on the 1:1 BA/isoNCT material (black) confirms that above 150 °C the spectrum observed for the 2:1 system is the same as that for the 1:1. Melting is subsequently observed at around 165 °C. These data are in good agreement with those obtained from XRD and HSM.

Thermogravimetric Analysis−Mass Spectrometry. To confirm the conversion of the 2:1 cocrystal to the 1:1 form, thermogravimetric analysis−mass spectrometry (TGA-MS) was performed. The results are shown in Figure 9. Mass loss is observed to commence at 80 °C. The mass spectrum shows clear signals at m/e = 51, 77, 105, and 122. These are typical of benzoic acid, thus confirming that BA is lost from the material. The material appears to decompose completely under these conditions, and it is not possible to ascertain with certainty where the conversion from 2:1 to 1:1 ends and when degradation begins. There does however appear to be a point of inflection at around 131−132 °C, where there is mass loss of 32.6%. The calculated loss for the conversion of BA_2/isoNCT to BA/isoNCT is 31%, in good agreement with this observed value.

Exploring the Transition Temperature. The data presented above clearly show the transformation of the 2:1 cocrystal into the 1:1 species upon heating, in accordance with the literature.[17,21] The transformation happens at different temperatures depending on the method of analysis used, which may be a result of sample size and shape variation. To investigate this further, a series of DSC and TGA experiments were performed. DSC data for the raw materials and both cocrystals are presented in Figure S9, Supporting Information. The DSC thermograms of the 1:1 cocrystal show a single endotherm corresponding to melting at 162.6 ± 0.17 °C. The 2:1 material exhibits a more complex thermogram, with an endotherm at 143.11 ± 0.14 °C followed by an exotherm and then a second endotherm. These data are in full agreement with the literature.[17,18,21] In a previous report,[17] it was suggested that the first endotherm corresponds to melting of the BA_2/isoNCT material followed by recrystallization of BA/isoNCT and finally the melting of the latter material. However, the HSM and XRD experiments presented above demonstrate that complete melting of the 2:1 cocrystal does not occur prior to the 1:1 system forming. We thus propose that the DSC events are more subtle than a simple melt/recrystallization and that the initial endotherm in the 2:1 DSC trace corresponds to the removal of BA from the structure. This will leave defects in the remaining structure, which then rearranges to give the 1:1 material in an exothermic process. The second endotherm is attributed to the 1:1 melt.

The effect of varying the heating rate on the BA_2/isoNCT transition temperature was next explored (see Figure 10).

DOI: 10.1021/acs.cgd.5b00351
Cryst. Growth Des. XXXX, XXX, XXX−XXX

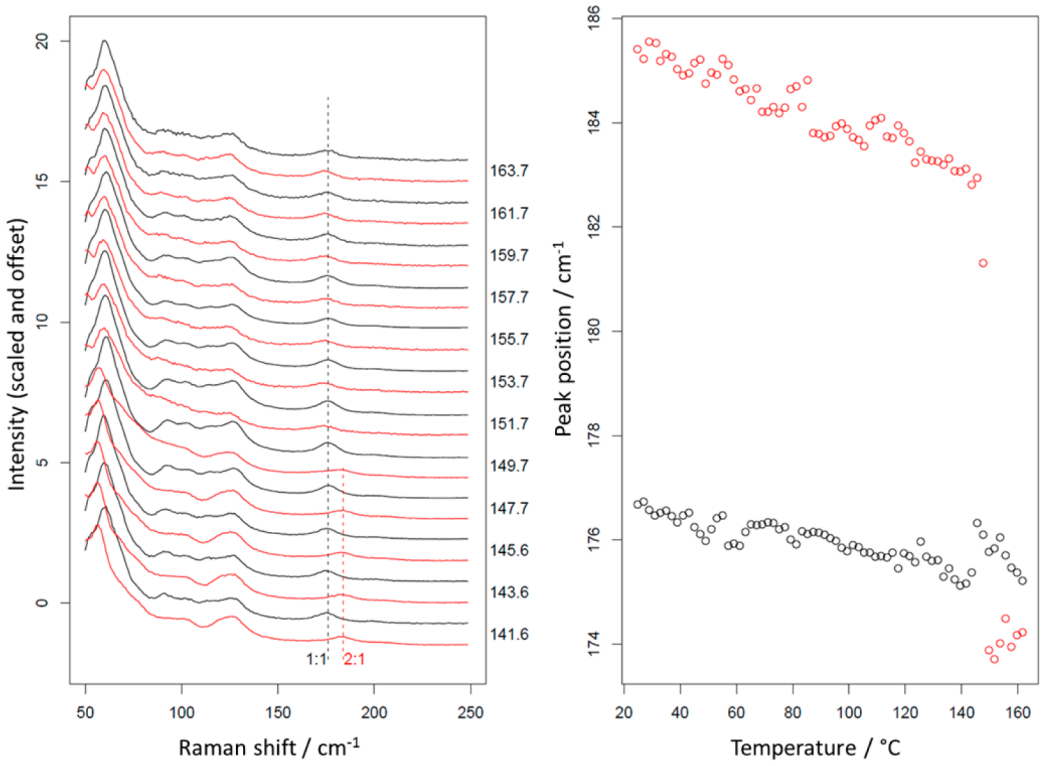

Figure 8. VT Raman data obtained on the BA/isoNCT and BA_2/isoNCT cocrystals. Data for the 2:1 material are shown in red and those for the 1:1 in black.

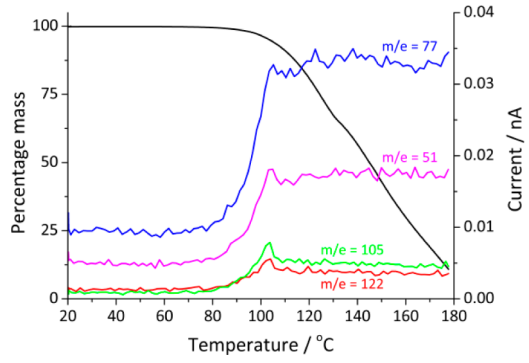

Figure 9. TGA-MS data recorded on the 2:1 BA_2/isoNCT cocrystal.

Increasing the heating rate has the effect of raising the extrapolated onset temperature at which the 2:1 to 1:1 transformation occurs in conventional DSC, from 140 °C at 2 °C min^{-1} to 141.6 ± 0.5 °C at 10 °C min^{-1} and 143 ± 0.5 °C at 100 °C min^{-1}. In rapid-heating DSC, two endotherms are visible at lower heating rates (presumably the first corresponds to the 2:1 → 1:1 transformation, and the second to the 1:1 melt). The extrapolated onset of the transformation endotherm moves from 142.7 ± 0.2 °C at 100 °C min^{-1} to 142.9 ± 0.2 °C (300 °C min^{-1}), 143.1 ± 0.6 °C (500 °C min^{-1}) and 140.7 ± 0.9 °C (1000 °C min^{-1}). At 1000 °C min^{-1}, the transformation and melt endotherms have merged. It is therefore clear that the heating rate of the sample influences the temperature at which

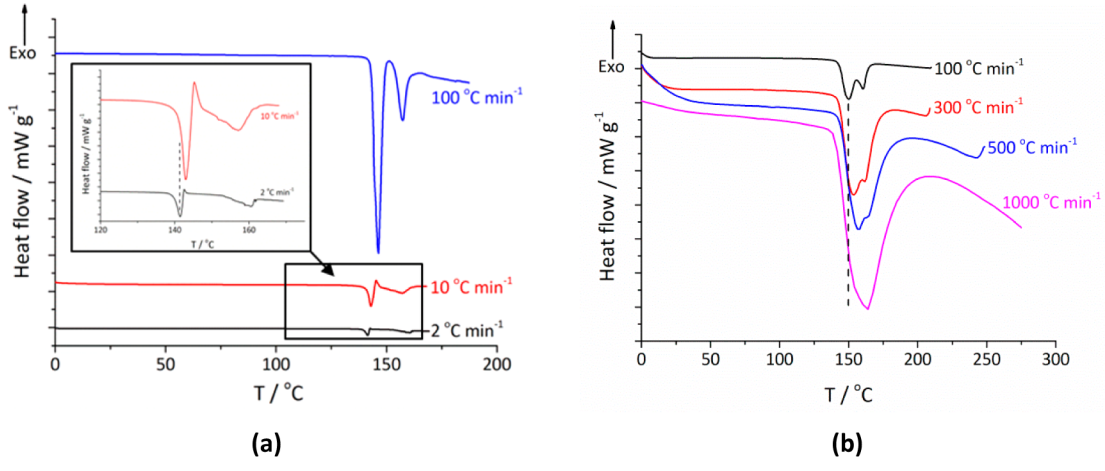

Figure 10. DSC data recorded on BA_2/isoNCT at different heating rates. Thermograms were obtained using (a) conventional DSC instrument and (b) rapid-heating DSC instrument.

DOI: 10.1021/acs.cgd.5b00351
Cryst. Growth Des. XXXX, XXX, XXX−XXX

the 2:1 to 1:1 transition occurs. This was verified by TGA experiments (see Figure S10, Supporting Information): the loss of BA from BA_2/isoNCT occurs at progressively higher temperatures as the heating rate is increased.

In addition, there are clear differences between the conventional DSC and RHC-DSC data during heating at 100 °C. The peak of the transformation endotherm is at very different temperatures in the two (146.3 °C in DSC and 150.1 °C in RHC-DSC), which is attributed to the variations in the size of the pan used between the two (the RHC-DSC uses pans of 1.6 mm in diameter and a sample size of just under 0.1 mg;[37] in contrast the Tzero pans used for DSC have an inner diameter of 5 mm and use a sample mass of ca. 5 mg). The effect of the pan was further explored by heating BA_2/isoNCT at 10 °C min^{-1} in conventional DSC using different pans; the results are presented in Figure S11, Supporting Information. The temperature at which the 2:1 to 1:1 transition occurs (T_{trans}) is clearly dependent on the sample geometry. T_{trans} is lower when an open Tzero pan is used than with a closed pan and is also lowered when using a hermetically sealed pan if a pinhole is made. This suggests that the removal of evolved gas from the crystal during transformation is very important: in open or pinholed pans, where the sublimed BA can more easily be carried away by the purge gas, the transformation happens at a lower temperature. The fact that an increased heating rate shifts T_{trans} to elevated temperatures is consistent with this: the removal of sublimed BA will be a kinetic process, and time is required to clear it after it has been evolved.

DISCUSSION

In this paper, a comprehensive collection of data obtained upon heating the 1:1 and 2:1 benzoic acid/isonicotinamide cocrystals is reported. Previous reports[17,18,21] have identified the existence a thermally mediated 2:1 to 1:1 transition using DSC and microscopy data. Here a range of *in situ* techniques have been utilized to explore the transition in more detail. Hot stage microscopy clearly shows that as the BA_2/isoNCT material is heated new crystals of BA/isoNCT begin to appear on its surface at around 85 °C, and by 120 °C the entire crystal has been completely transformed. *In situ* synchrotron diffraction reveals that, while BA/isoNCT shows only an expansion in its *a* parameter when heated, BA_2/isoNCT exhibits much more significant changes. Both its *a* and *c* parameter expand rapidly as the temperature rises, and above 140 °C, it appears that a two-phase mixture of materials is present, with a smaller unit cell evolving. Above 160 °C, the pattern has completely changed, and a partial Rietveld fit using the BA/isoNCT structure confirms that the 2:1 material is completely transformed to the 1:1. The unit cells calculated at 161 °C are essentially identical, regardless of which cocrystal was present before heating commenced. The changes observed in the 2:1 diffraction pattern before the transformation occurs can be rationalized by a consideration of the intermolecular bonding in the two structures: the expansion in the *c* direction arises from a weakening of C−H···π interactions in the 2:1 system. This causes the BA−isoNCT−BA slabs (see Figure 1) to move apart, creating space and facilitating the departure of BA molecules to yield the 1:1 material. The HSM data show that gas bubbles are evolved from the structure, consistent with this hypothesis.

The transition from 2:1 to 1:1 stoichiometry is verified by *in situ* Raman spectroscopy (where very clear changes in the spectrum occur upon heating, consistent with formation of BA/isoNCT) and also by TGA-MS, in which BA is clearly present in the purge gas. It is thus conclusively demonstrated that BA_2/isoNCT loses BA to form BA/isoNCT when it is subjected to heating.

The reason this transformation occurs can be understood by a simple consideration of the thermodynamics in the two materials. There will be a significant increase in entropy when the conversion occurs, as a result of the freeing of an equivalent of gaseous BA. There is also likely to be an enthalpic contribution to the Gibbs free energy of the transformation. BA/isoNCT contains classical H-bonds, which dominate the intermolecular interactions. BA_2/isoNCT also possesses some H-bonds, but there are in addition many much weaker C−H···π interactions. More H-bonds are possible in the BA/isoNCT material. The existence of a 2:1 to 1:1 transformation agrees with the equations calculated for the free energy of formation of BA/isoNCT cocrystals by Sangster; these show the 1:1 cocrystal to be more thermodynamically stable than the 2:1 under all the conditions used in this work.[23]

This therefore permits explanation of why the 2:1 → 1:1 transition arises at different temperatures in different experiments. *In situ* diffraction experiments use a relatively large volume of sample, but the culture tube used for reaction is only 9 mm in internal diameter. Most of the sample surface is confined by glass; it is thus difficult for the BA to escape from the material, and a high transformation temperature (T_{trans}) is observed. In contrast, in HSM, the crystals are very loosely packed with BA gas able to escape easily from any part of any crystal, leading to a lower T_{trans}. A similarly low T_{trans} is notable in the TGA-MS data, conducted in an open pan with a flow of gas. In DSC and TGA experiments, T_{trans} moves to higher temperatures with more rapid heating rates. The use of open DSC pans (or those with pin-holes) results in lower T_{trans} than when the pans are sealed. These effects can be explained because there is likely to be an equilibrium between gaseous BA and BA in the crystal structure. A gas flow aids the movement of gaseous BA away from the crystals, shifting this equilibrium in favor of BA/isoNCT.

CONCLUSIONS

A range of *in situ* techniques have been implemented to study the thermal behavior of the 2:1 and 1:1 benzoic acid/isonicotinamide cocrystals. Building on earlier studies, we have performed detailed hot-stage microscopy, time-resolved X-ray diffraction, differential scanning calorimetry, and thermogravimentric analysis−mass spectrometry experiments to thoroughly characterize these systems, the thermal behavior of which has previously not been studied in detail. The 1:1 system shows a simple thermal expansion of the unit cell, followed by melting. The 2:1 crystal shows more interesting behavior and is converted to the 1:1 system upon heating. This transition begins at the surface of the crystals. It is preceded by significant changes in the unit cell, which can be rationalized in terms of the breaking of C−H···π interactions required to convert the 2:1 to the 1:1 stoichiometry. The evolution of benzoic acid is clearly evidenced by combined thermogravimetric analysis−mass spectrometry. The temperature at which the phase transition occurs is highly dependent on the sample environment and is reduced when the uncovered surface area is increased or with a flow of gas. This temperature increases with faster heating rates. There is believed to exist an equilibrium between benzoic acid (BA) in the 2:1 crystal and evolved BA gas, and hence the more rapidly the sublimed BA is cleared

DOI: 10.1021/acs.cgd.5b00351
Cryst. Growth Des. XXXX, XXX, XXX−XXX

from the cocrystal surface the lower the temperature at which the transformation occurs.

■ ASSOCIATED CONTENT

Supporting Information

An enlargement of Figure 2, additional HSM images, Rietveld fits to selected time-resolved XRD datasets, comparisons of XRD patterns collected from the 1:1 and 2:1 cocrystals at different temperatures, and additional DSC and TGA data. The Supporting Information is available free of charge on the ACS Publications website at DOI: 10.1021/acs.cgd.5b00351.

■ AUTHOR INFORMATION

Corresponding Authors

*S.G. E-mail: s.gaisford@ucl.ac.uk. Tel: +44 (0) 20 7753 5853.
*G.R.W. E-mail: g.williams@ucl.ac.uk. Tel: +44 (0) 207 753 5868.

Notes

The authors declare no competing financial interest.

■ ACKNOWLEDGMENTS

The authors gratefully thank the Diamond Light Source for access to Beamline I12 (EE7782-1), Professor Dermot O'Hare and Dr. Saul Moorhouse (University of Oxford) for access to ODISC, Dr. Christina Reinhard (Diamond) for help and support with experiments on I12, Dr. David Berry (Durham University) and Prof. Nicolas Blagden (Lincoln University) for support in collecting the hot-stage microscopic data, and Mr. Alexander Prior for helpful discussions.

■ REFERENCES

(1) Blagden, N.; Coles, S. J.; Berry, D. J. *CrystEngComm* **2014**, *16*, 5753−5761.
(2) Stahl, P. H.; Wermuth, C. G. *Pharmaceutical Salts: Properties, Selection, and Use*, 2nd ed.; Wiley VCH: Weinheim, Germany, 2011.
(3) Brittain, H. G. *J. Pharm. Sci.* **2011**, *100*, 1260−1279.
(4) Sun, C. C. *Expert Opin. Drug Delivery* **2013**, *10*, 201−213.
(5) Trask, A. V.; Motherwell, W. D. S.; Jones, W. *Int. J. Pharm.* **2006**, *320*, 114−123.
(6) McNamara, D. P.; Childs, S. L.; Giordano, J.; Iarriccio, A.; Cassidy, J.; Shet, M. S.; Mannion, R.; O'Donnell, E.; Park, A. *Pharm. Res.* **2006**, *23*, 1888−1897.
(7) Banerjee, R.; Bhatt, P. M.; Ravindra, N. V.; Desiraju, G. R. *Cryst. Growth Des.* **2005**, *5*, 2299−2309.
(8) Sun, C. C.; Hou, H. *Cryst. Growth Des.* **2008**, *8*, 1575−1579.
(9) Karki, S.; Friscic, T.; Fabian, L.; Laity, P. R.; Day, G. M.; Jones, W. *Adv. Mater.* **2009**, *21*, 3905−3909.
(10) Cheyney, M. L.; Weyna, D. R.; Shan, N.; Hanna, M.; Wojitas, L.; Zaworotko, M. J. *J. Pharm. Sci.* **2011**, *100*, 2172−2181.
(11) Tothadi, S.; Desiraju, G. R. *Chem. Commun.* **2013**, *49*, 7791−7793.
(12) Habgood, M. *Cryst. Growth Des.* **2013**, *13*, 4549−4558.
(13) Habgood, M.; Deij, M. A.; Mazurek, J.; Price, S. L.; ter Horst, J. H. *Cryst. Growth Des.* **2010**, *10*, 903−912.
(14) Habgood, M.; Price, S. L. *Cryst. Growth Des.* **2010**, *10*, 3263−3272.
(15) Mohamed, S.; Tocher, D. A.; Price, S. L. *Int. J. Pharm.* **2011**, *418*, 187−198.
(16) Issa, N.; Barnett, S. A.; Mohamed, S.; Braun, D. E.; Copley, R. C. B.; Tocher, D. A.; Price, S. L. *CrystEngComm* **2012**, *14*, 2454−2464.
(17) Buanz, A. B. M.; Telford, R.; Scowen, I. J.; Gaisford, S. *CrystEngComm* **2013**, *15*, 1031−1035.
(18) Seaton, C. C.; Parkin, A.; Wilson, C. C.; Blagden, N. *Cryst. Growth Des.* **2009**, *9*, 47−56.
(19) Boyd, S.; Back, K.; Chadwick, K.; Davey, R. J.; Seaton, C. C. *J. Pharm. Sci.* **2010**, *99*, 3779−3786.
(20) Croker, D. M.; Davey, R. J.; Rasmuson, Å. C.; Seaton, C. C. *CrystEngComm* **2013**, *15*, 2044−2047.
(21) Seaton, C. C.; Parkin, A.; Wilson, C. C.; Blagden, N. *Cryst. Growth Des.* **2008**, *8*, 363−368.
(22) Aakeröy, C. B.; Beatty, A. M.; Helfrich, B. A. *Angew. Chem., Int. Ed.* **2001**, *40*, 3240−3242.
(23) Sangster, J. *J. Phys. Chem. Ref. Data* **1999**, *28*, 889−930.
(24) Jung, S.; Ha, J.-M.; Kim, I. *Polymers* **2013**, *6*, 1−11.
(25) Reddy, L. S.; Bhatt, P. M.; Banerjee, R.; Nangia, A.; Kruger, G. J. *Chem.—Asian. J.* **2007**, *2*, 505−513.
(26) Bevill, M. J.; Vlahova, P. I.; Smit, J. P. *Cryst. Growth Des.* **2014**, *14*, 1438−1448.
(27) Alhalaweh, A.; George, S.; BostrÖm, D.; Velaga, S. P. *Cryst. Growth Des.* **2010**, *10*, 4847−4855.
(28) Eddleston, M. D.; Lloyd, G. O.; Jones, W. *Chem. Commun.* **2012**, *48*, 8075−8077.
(29) Aitipamula, S.; Wong, A. B. H.; Chow, P. S.; Tan, R. B. H. *CrystEngComm* **2012**, *14*, 8193−8198.
(30) http://www.diamond.ac.uk/Home/Beamlines/I12.html.
(31) Moorhouse, S. J.; Vranjes, N.; Jupe, A.; Drakopoulos, M.; D, O. H. *Rev. Sci. Instrum.* **2012**, *83*, No. 084101.
(32) Hammersley, A. P. ESRF Internal Report 1998, ESRF98HA01T, FIT2D V9.129 Reference Manual V3.1.
(33) Hammersley, A. P.; Svensson, S. O.; Hanfland, M.; Fitch, A. N.; Haeusermann, D. *High Pressure Res.* **1996**, *14*, 235−248.
(34) Larson, A. C.; Von Dreele, R. B. Los Alamos National Laboratory Report 1994, General Structure Analysis System (GSAS).
(35) Al-Dulaimi, S.; Aina, A.; Burley, J. *CrystEngComm* **2010**, *12*, 1038−1040.
(36) Brillante, A.; Bilotti, I.; Della Valle, R. G.; Venuti, E.; Girlando, A. *CrystEngComm* **2008**, *10*, 937−946.
(37) Danley, R.; Caulfield, P.; Aubuchon, S. *Am. Lab.* **2008**, *40*, 9−11.

DOI: 10.1021/acs.cgd.5b00351
Cryst. Growth Des. XXXX, XXX, XXX−XXX